Aalborg Universitet

AALBORG UNIVERSITY
DENMARK

Cycle-life of Li-ion Capacitors: Factors Influencing Aging

Saha, Pankaj; Soltani, Mahdi; Munk-Nielsen, Stig; Stroe, Daniel-Ioan

Cycle-life of Lithium-ion Capacitors: Factors Influencing Aging

1st Pankaj Saha
Department of Energy
Aalborg University
Aalborg, Denmark
psa@energy.aau.dk

2nd Mahdi Soltani
Department of Energy
Aalborg University
Aalborg, Denmark
maso@energy.aau.dk

3rd Stig Munk-Nielsen
Department of Energy
Aalborg University
Aalborg, Denmark
smn@energy.aau.dk

4th Daniel-Ioan Stroe
Department of Energy
Aalborg University
Aalborg, Denmark
dis@energy.aau.dk

Abstract—**A comprehensive study of the factors influencing the cycle life of Lithium-ion capacitors (LICs) at different stages of aging is essential for a promising LIC energy management system. This paper studies the factors influencing the aging of LICs. The commercially available 2100F Musashi LIC cells are chosen to perform cyclic aging experiments under different test conditions. The test matrix includes different temperatures (40^oC, 50^oC), charge-discharge rates (C-rate) ($4C, 53C$), and depth of discharge (DoD) levels ($100\%, 60\%$). The results indicate that C-rate is inversely proportional to the capacitance degradation of LIC. At a low C-rate, both the cyclic aging and calendar aging component contributes to the cell's degradation. Similarly, temperature and DoD significantly influence the degradation of the LIC, and both are linearly related to aging. However, these parameters are highly sensitive to the other operating conditions of the cells. Finally, the Arrhenius equation has been applied to the test results and qualitatively analyzed the LIC degradation mechanism.**

Index Terms—**Lithium-ion capacitor (LIC), accelerated aging, cycle-life, activation energy, state of health**

I. Introduction

Lithium-ion Capacitors (LICs) store energy by combining the charge adsorption technology of electric double-layer capacitors (EDLCs) with the charge intercalation technology of lithium-ion batteries (LIBs). Such a hybrid energy storage system merges the advantages of both EDLC and LIB technologies, including high power density ($\sim$ 14kW/kg), high energy density ($\sim$ 45Wh/kg), long cycle life ($> 300,000$ cycles), and wide operating temperature range (-20°C to 70°C) [1]. These unique properties of LIC have led to wide range of applications, for example, power electronics applications [2], wind power generation [3], lightweight transportation systems [4], regenerative braking systems [5], pulse power applications [6], electric vehicles [7], etc. Another promising application of LIC could be the grid stability control by primary frequency regulation, as demonstrated in [8].

Given the broad application spectrum, the aging characterization of such an emerging storage technology is crucial, especially for its energy management. LIC aging characterization can be broadly divided into two groups: (i) characterization that attempts to simulate calendar aging of the cell under different floating voltages and temperatures [9], [10], and (ii) characterization that studies the cyclic aging of the cell under different charge-discharge rates (C-rates), depth of discharge (DoD), and operating temperatures [11]–[14]. In this paper, the authors aim to assess the performance degradation behavior of LIC cells under cycle aging at various conditions of temperature, C-rate, and cycle depths. A number of studies have been reported in the literature focused on the cyclic aging characterization of LIC, considering various realistic applications and operating conditions [11]–[13]. Cycle life evaluation of LICs as an alternative to Li-ion batteries for spacecraft power systems is studied in [13]. The study concludes that, unlike LIBs and EDLCs, the aging acceleration factor of LIC is not constant, and the cell degradation mechanism is independent of test conditions; however, the degradation rate is a function of the test conditions. Furthermore, the identified activation energy is not the same for the cells from different manufacturers; hence, their degradation mechanism. The physics-based model of LIC proposed in [14] studied the significant degradation mechanics that caused the capacity loss at most in reality. From the hybrid storage system viewpoint, various degradation mechanisms occur in LIC, including loss of active material, loss of Lithium-ion inventory (LLI), and precipitation of electrolyte salt. The effects of multiple or coupled degradation mechanisms result in LICs' capacitance fade and internal resistance evolution; consequently, the degradation rate is not the same during the entire lifetime of the cell. For Lithium-ion intercalation mechanism-based energy storage systems, ideally, the degradation rate is higher at the initial accelerated aging stage than at the stabilization stage, and it reaches its maximum during the saturation phase [15]. A data-driven LIC lifetime prediction model is proposed in [11] for both the cyclic and calendar aging conditions under different temperatures. Another empirical model for LIC cyclic life has been proposed in [12], in the context of a LIC-equipped standalone PV system. These proposed models determine the state of health of the LIC as a function of its aging parameters and estimate the end-of-life by extrapolating the available experimental results. These proposed cycle life characterization schemes generalize the impacts of test/aging conditions over the entire lifetime of the cells. This paper focuses on characterizing the effect of aging parameters on the

LIC cell's state of health. In particular, (i) the influence of C-rates, DoDs, and temperatures on the cyclic aging of the LIC; and (ii) a qualitative analysis of the degradation mechanisms.

The remainder of this paper is organized as follows. The experimental detail, including the LIC specification, test matrix, and characterization methods, are discussed in Section II. The experimental results of the accelerated aging tests performed under different conditions and the analysis of those results are presented in Section III. Finally, Section IV concludes this paper.

II. EXPERIMENTAL: TEST SETUP, TEST MATRIX, AND CHARACTERIZATION

Test setup - The experiments have been conducted on the commercially available 2100F LIC cells from Musashi Energy Solutions. The cell material comprises an SC-like activated carbon electrode as the cathode and a LIB-like carbon anode. The cell specifications are listed in Table I. All the aging tests related to the cycle-life characterization of the cells are performed using the following set of equipment: (i) Digatron testing module with a maximum current supply of 50A and a voltage output of 6V, featuring a measurement accuracy of 0.1% of the full range; (ii) Memmert climatic chamber with a controlled ambient temperature ranging from -12°C to 60°C; and (iii) Temperature sensor of K-type thermocouple accurate to $\pm 0.5^o$C. Battery management software, BTS600, is used to design cyclic aging profiles and acquire data at a rate of 1Hz. The cells are mounted on a solid base made from a thermoplastic sheet to increase the delicate terminals' mechanical strength and act as insulation between the terminals and the metal rack inside the climate chamber. Fig. 1 shows the whole setup.
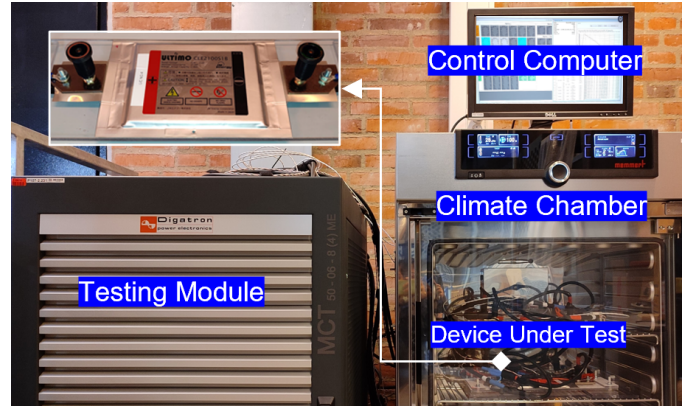

Fig. 1. Experimental setup

Ambient Temp.	Depth-of-Discharge (DoD)				C-rate
	100%		60%		
40°C		12960 (L2)		11733 (L4)	4C
	140775 (L1)		116320 (L3)		53C
50°C	6900 (L5)		10938 (L6)		4C
		79000 (L8)			53C
	13000 (L7)				10C

Fig. 2. Accelerated aging test matrix

TABLE I
MUSASHI CLE2100S1B ULTIMO LITHIUM-ION CAPACITOR SPECIFICATION [16]

Parameter	Value
Rated, Nominal voltage	$2.2 - 3.8V, 3.0V$
Capacitance, Capacity	2100 F, 0.93Ah
Energy density	24 Wh/kg
Power density	4 kW/kg
Temperature range	-20^oC to 70^oC
Projected cycle life	$> 300,000$ cycles

Accelerated aging test matrix - The aging tests of the LIC cells are performed under the specific conditions mentioned in Fig. 2. The test parameters include two different ambient temperatures (40°C and 50°C), two different C-rates (4C and 53C), and two different levels of DoD (60% and 100%). One cell is tested under each specified test condition; thus, eight cells are tested. The current value corresponding to the 4C and 53C is re-defined to 3.75A and 50A, respectively, in performing the cyclic aging in constant-current (CC) mode. The voltage intervals for the 100% and 60% DoDs are 3.8-2.2V and 3.8-2.88V, respectively. The lower cut-off voltage for the latter has been experimentally identified via open circuit voltage vs. SOC mapping of the cell, shown in Fig. 3. Several factors are

taken into account when selecting the aging test conditions: discharge rates of energy storage systems integrating with grid frequency regulation and transport electrification; accelerated aging within the operating temperature range; aging responses for identical LIC cells are given in the datasheet.

The numbers in the test matrix represent cycles performed by the cells under each condition. The corresponding cell IDs (namely L1, L2,..., L8) are mentioned in the round brackets below the cycle number. In addition, this study also considers the aging test results reported in the technical data sheet of three identical Musashi cells [16]. Their test conditions include an ambient temperature of 25°C, a DoD of 100%, and three C-rates of 4C, 10C, and 53C. These three cells will be referred to as D1 (4C), D2 (53C), and D3 (10C) throughout this paper.

Characterization - The cyclic aging involves periodically stopping the cells for performance characterization, namely reference performance test (RPT). The reference performance test, which consists of capacity (in Ampere-hour), capacitance (in Farad), and DC-IR (in Ω) measurements of the cells at 25°C, has been performed following the IEC 62813:2015 international standards defines the electrical characteristics of LIC [17]. The reference performance tests of the LIC cells are
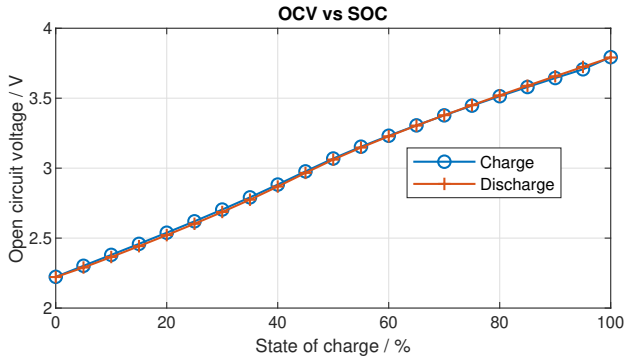
Fig. 3. State of charge (SOC) vs. open circuit voltage (OCV) relationship of Musashi LIC

performed every two weeks between cyclic aging tests.

III. RESULTS AND DISCUSSION

The aging test matrix (shown in Fig. 2) comprehending temperature, DoD, and C-rate allows a statistical analysis of the factors that affect LIC's cycle life, i.e., state of health. Fig. 4 shows the capacity retention of the LICs as a function of the equivalent full cycle[1] (EFC) at different temperatures, C-rates, and DoDs. Based on the C-rate and DoD, the LICs completed different numbers of aging cycles at the time of writing this paper. L1 performed the highest number of EFCs, 140775 cycles, and L5 performed the lowest number, 6900 cycles. However, except for cell L7, none of the LICs reached their end-of-life criteria, i.e., a 20% capacitance drop from their initial value.
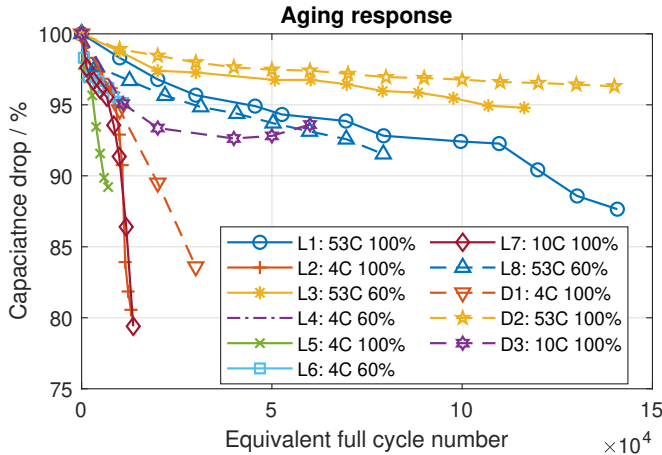

Fig. 4. Capacitance retention at different temperature (25^oC, 40^oC, 50^oC), depth of discharge (100%, 60%), and charge-discharge rate (4C, 53C) plotted as a function of equivalent full cycles

[1]The equivalent full cycle of a LIC cell defines the number of complete charge-discharge cycles calculated from the ampere-hour (Ah) throughput after the charge-discharge operation of the cell, defined as $N_E = \frac{T_{ah}}{2C_{ah}}$, where N_E denotes the number of the equivalent full cycles performed, T_{ah} denotes the ampere-hour throughput after the end of the charge-discharge operations, and C_{ah} denotes the Ah capacity of the cell.

In the following subsections, the effect of C-rate, DoD, and temperature on the LIC cells are discussed in detail. As mentioned earlier that the cells undergo different aging cycles; therefore, their complete EFCs were not taken into consideration for comparing the influence of aging parameters on the cells. The number of EFCs for a particular study has been determined by the LIC cell with the most EFCs completed. This can be seen from Fig. 5(a), (c), and (e).

A. Effect of C-rate

At a given DoD, cells cycled at a lower C-rate experienced equivalent degradation sooner than those at a higher C-rate, as shown in Fig. 4. Fig. 5(a),(c), and (e) separately plot the capacitance retention of the cells as a function of the equivalent full cycle (EFC) at different C-rates, 4C, 53C, and 10C, respectively. The average degradation of the LICs aging at 53C after 79000 EFCs is 5.66%, while the cells aging at 4C degraded almost the same (on average 5.19%) after only 6900 EFCs. A similar observation is seen for LICs aging at 10C. This result demonstrates that C-rate significantly impacts LIC's cycle life, which is inversely proportional; as the C-rate decreases, the rate of capacitance drop increases and vice versa. Alongside, the capacitance fades are plotted as a function of their aging duration, as shown in figure 5(b),(d), and (f). It shows that the cells aged at a low C-rate undergo charge-discharge operations more than those at a higher C-rate. Consequently, the calendar-aging component contributes more to the overall aging of the cells cycling at 4C and 10C than 53C. This justifies the above-mentioned inversely proportional relationship between the C-rate and the EFC of the cells.

B. Effect of DoD

Next, cells cycled at different DoDs at a given C-rate and temperature are studied. Fig. 6 compares the percentage of capacity loss of the cells cycled at the same temperature and C-rate, however, at different DoDs. A close examination of the results shows that the percentage capacitance drop among cells L1 and L3 differ at a given C-rate and temperature. There is a loss of 7.15% of capacitance in Cell L1 at 100%DoD and 4.03% in Cell L3 at 60%DoD. A similar phenomenon can be observed between L5 and L6. At 100%DoD, L5 loses 10.75% of its capacitance, while L6 loses just 3.8% at 60%DoD. Interestingly, the capacitance drop observed between L2 and L4 is almost the same, although their DoDs are different, 100% and 60%, respectively. So, it can be observed that the state of health of the LIC is also affected by the DoD levels; however, the impact of DoD is sensitive to C-rate and ambient temperature. When both the ambient temperature and C-rate are low, the impact of the DoD level is less significant on the health degradation of the cell; otherwise, DoD is linearly related to aging.

C. Effect of temperature

In Fig. 7, the percentage of capacity loss is plotted as a function of the cell temperature. For a given C-rate and DoD, it is observed that the percentage of capacitance drop
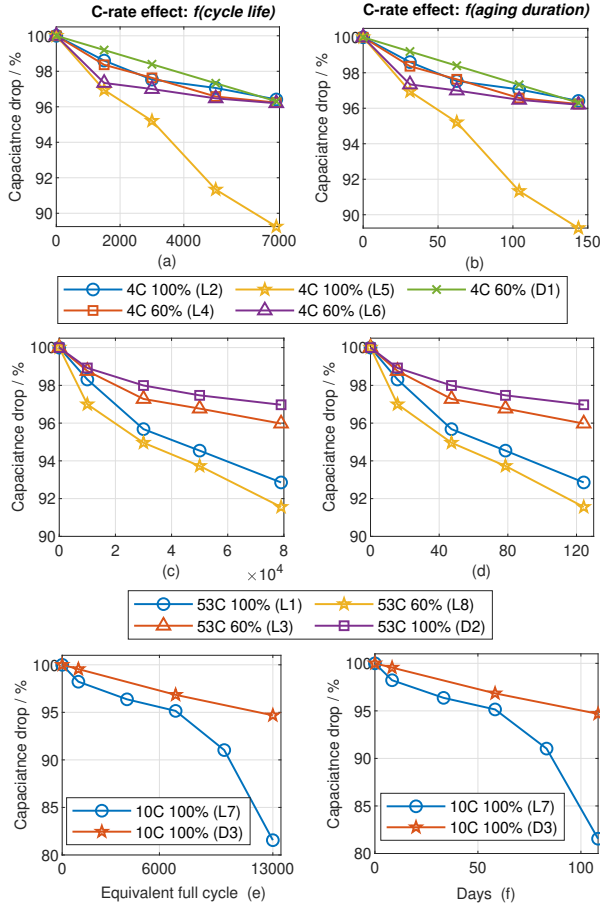
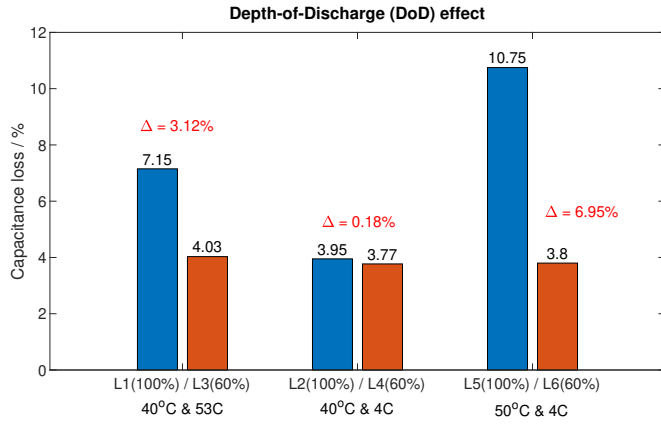Fig. 5. Capacitance retention as a function of (a,c,e) equivalent full cycle and (b,d,f) aging duration

Fig. 6. Capacitance degradation as a function of depth of discharge (DoD)

is linearly related to the cell temperature. After 79000 cycles, D2 loses 3.03% of capacitance at 25^oC, while L1 loses 7.15% of its initial capacitance at 40^oC. In the case of cells D1 and L2, the percentage of capacitance drop corresponding to the cell temperatures 25^oC and 40^oC are 3.7% and 3.95%, respectively. As the ambient temperature increases, the rate of health degradation also increases. While L8 experiences a capacity drop of 8.45% after 79000 cycles at 50^oC, the capacitance drop of L3 is limited with 4.03% after the same number of cycles at 40^oC. Similarly, D3 and L7 lose 5.32% and 18.45% of their initial capacitance after 13000 cycles at 25^oC and 50^oC, respectively. Furthermore, it can be observed that the impact of temperature on aging is sensitive to the C-rate and DoD level of the LIC cells.
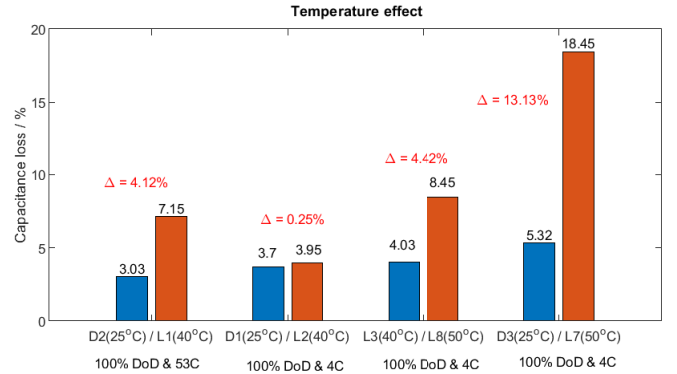

Fig. 7. Capacitance degradation as a function temperature

D. Activation energy of the degradation dynamics

Finally, a qualitative analysis of the cell degradation trend has been conducted. Following a similar approach studied in [13], the activation energy of the capacitance degradation was identified using the Arrhenius equation, as defined below.

$$logC_L = \frac{1}{2.303}\frac{-E_a}{1000R}\frac{1000}{T} + logK, \qquad (1)$$

where C_L denotes percentage of capacitance loss, E_a denotes activation energy, R denotes gas constant, T denotes cell temperature, and K denotes a coefficient. The activation energy characterizes the aging dynamics of the cell. In determining the activation energy, the Arrhenius equation is applied to the capacitance degradation trends of the cells at the given C-rate. Fig. 8 shows the identified best-fitted Arrhenius plot trend of the cells. It can be observed that there are a few instances where the relationship between $log(C_L)$ and $\frac{1000}{T}$ can't be accurately characterized by the linear line with a slope of $-E_a$; the different DoD levels of the LICs could be a reason for this nonlinearity. One direction of future work is to consider the DoD parameter in the Arrhenius equation defined in (1) and characterize the capacitance degradation more accurately.

Fig. 9 shows the activation energy trends obtained from the best-fitted values determined by the MATLAB curve fitting toolbox. The activation energy trends of the cells D2-L1-L3-L8, shown in Fig. 9(a), are almost independent of the cyclic

condition. However, D1-L2-L4 and D2-L7 reflect different activation energy trends under different cyclic conditions, as shown in Fig. 9(b) and (c), respectively. Different trends in activation energies indicate (i) varying capacitance degradation rates and (ii) non-homogeneous degradation reactions during different aging cycles.
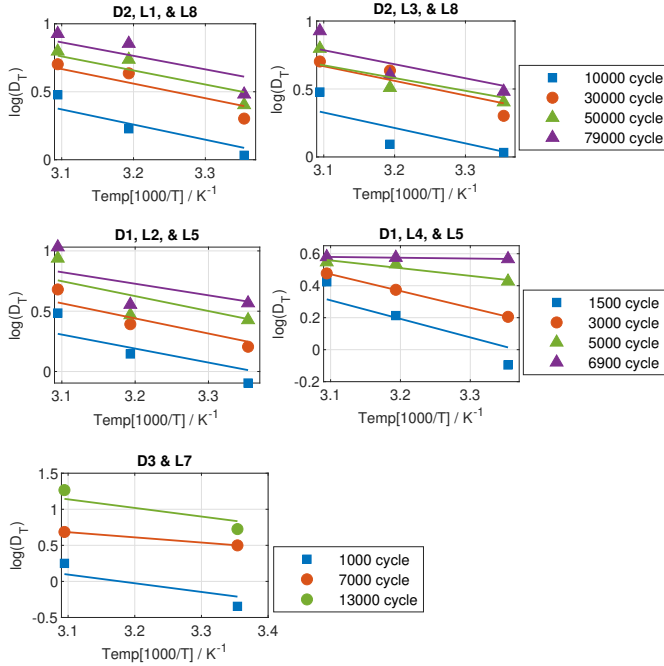

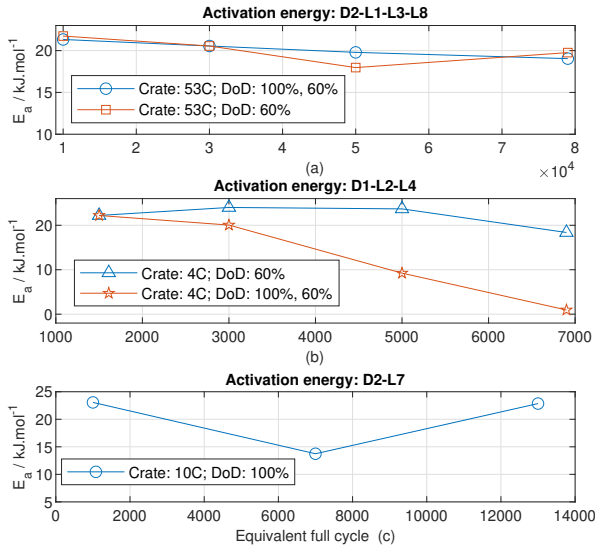Fig. 8. Arrhenius plot trends of LICs under different aging conditions

Fig. 9. Activation energy trends of LICs under different aging conditions

IV. CONCLUSION

This paper presents the intermediate results of an ongoing cyclic aging test from an accelerated aging cycle study on commercially available 2100F Musashi LIC cells. The effects of test parameters, including temperature, C-rate, and DoD, on aging, are investigated and analyzed. Results indicate that cell C-rate strongly influences capacitance degradation and that C-rate is inversely related to cycle life. Cells cycling at low C-rates experience both cyclic and calendar aging. Besides, temperature and DoD are linearly related to the capacitance degradation of the cell. As opposed to general trends, DoD has been found to impact the initial stage of aging significantly. However, the impact of DoD and temperature on aging is highly sensitive to the other aging parameters. Finally, the capacitance degradation trends have been studied qualitatively. In that direction, the Arrhenius equation is applied to the capacitance degradation ratios to determine the activation energies of the cell degradation mechanism. For the same C-rate, the different activation energy implies a varying aging trend of the cells. The varying trends of activation energies infer a non-homogeneous degradation mechanism in the tested aging period.

REFERENCES

[1] M. Soltani and S. H. Beheshti, "A comprehensive review of li-ion capacitor:development, modelling, thermal management applications," *Journal of Energy Storage*, vol. 34, p. 102019, 2021.

[2] S. Lambert, V. Pickert, J. Holden, X. He, and W. Li, "Comparison of supercapacitor and lithium-ion capacitor technologies for power electronics applications," in *5th IET international conference on power electronics, machines and drives (PEMD 2010)*. IET, 2010, pp. 1–5.

[3] S. A. Hamidi, E. Manla, and A. Nasiri, "Li-ion batteries and li-ion ultracapacitors: Characteristics, modeling and grid applications," in *2015 IEEE Energy Conversion Congress and Exposition (ECCE)*. IEEE, 2015, pp. 4973–4979.

[4] F. Ciccarelli, G. Clemente, D. Iannuzzi, and D. Lauria, "An analytical solution for optimal design of stationary lithium-ion capacitor storage device in light electrical transportation networks," *International Review of Electrical Engineering*, vol. 8, no. 3, pp. 989–999, 2013.

[5] D. Karimi, H. Behi, J. Van Mierlo, and M. Berecibar, "A comprehensive review of lithium-ion capacitor technology: Theory, development, modeling, thermal management systems, and applications," *Molecules*, vol. 27, no. 10, p. 3119, 2022.

[6] R. B. Sepe, A. Steyerl, and S. P. Bastien, "Lithium-ion supercapacitors for pulsed power applications," in *2011 IEEE Energy Conversion Congress and Exposition*. IEEE, 2011, pp. 1813–1818.

[7] M. Soltani, J. Ronsmans, S. Kakihara, J. Jaguemont, P. Van den Bossche, J. Van Mierlo, and N. Omar, "Hybrid battery/lithium-ion capacitor energy storage system for a pure electric bus for an urban transportation application," *Applied sciences*, vol. 8, no. 7, p. 1176, 2018.

[8] D.-I. Stroe, V. Knap, M. Swierczynski, A.-I. Stroe, and R. Teodorescu, "Operation of a grid-connected lithium-ion battery energy storage system for primary frequency regulation: A battery lifetime perspective," *IEEE Transactions on Industry Applications*, vol. 53, no. 1, pp. 430–438, 2016.

[9] S. Song, X. Zhang, Y. An, T. Hu, C. Sun, L. Wang, C. Li, X. Zhang, K. Wang, Z. J. Xu *et al.*, "Floating aging mechanism of lithium-ion capacitors: Impedance model and post-mortem analysis," *Journal of Power Sources*, vol. 557, p. 232597, 2023.

[10] N. El Ghossein, A. Sari, P. Venet, S. Genies, and P. Azaïs, "Post-mortem analysis of lithium-ion capacitors after accelerated aging tests," *Journal of Energy Storage*, vol. 33, p. 102039, 2021.

[11] M. Soltani, J. Ronsmans, and J. Van Mierlo, "Cycle life and calendar life model for li-ion capacitor technology in a wide temp. range," *Journal of Energy Storage*, vol. 31, p. 101659, 2020.

[12] T. Ibrahim, T. Kerekes, D. Sera, and D.-I. Stroe, "Degradation behavior analysis of high energy hybrid li-ion capacitors in stand-alone pv applications," in *IECON 2022–48th Annual Conference of the Industrial Electronics Society*. IEEE, 2022, pp. 1–6.

[13] M. Uno and A. Kukita, "Cycle life evaluation based on accelerated aging testing for li-ion capacitors as alternative to rechargeable batteries," *IEEE Transactions on Industrial Electronics*, vol. 63, no. 3, pp. 1607–1617, 2015.

[14] G. Madabattula, B. Wu, M. Marinescu, and G. Offer, "Degradation diagnostics for li4ti5o12-based lithium ion capacitors: Insights from a physics-based model," *Journal of the Electrochemical Society*, vol. 167, no. 4, p. 043503, 2020.

[15] J. S. Edge, S. O'Kane, R. Prosser, N. D. Kirkaldy, A. N. Patel, A. Hales, A. Ghosh, W. Ai, J. Chen, J. Yang *et al.*, "Lithium ion battery degradation: what you need to know," *Physical Chemistry Chemical Physics*, vol. 23, no. 14, pp. 8200–8221, 2021.

[16] Musashi Energy Solution Co.,Ltd., "Ultimo CLE2100S1B Li-ion Capacitor Technical Data Sheet", https://musashi-es.co.jp/en/products/cell-rami.html, accessed Feb 11, 2023.

[17] IEC 62813:2015 Edition 1.0 2015-01, "Lithium ion capacitors for use in electric and electronic equipment – Test methods for electrical characteristics", https://webstore.iec.ch/publication/7441.